

# Lawrence Berkeley National Laboratory

## Bldg Technology Urban Systems

### Title

Coupling CFD and building energy modelling to optimize the operation of a large open office space for occupant comfort

### Permalink

<https://escholarship.org/uc/item/1dm7x34h>

### Authors

Shan, Xiaofang

Luo, Na

Sun, Kaiyu

et al.

### Publication Date

2020-09-01

### DOI

10.1016/j.scs.2020.102257

Peer reviewed

# **Coupling CFD and Building Energy Modeling to Optimize the Operation of a Large Open Office Space for Occupant Comfort**

Xiaofang Shan <sup>a</sup>, Na Luo <sup>b</sup>, Kaiyu Sun <sup>b</sup>, Tianzhen Hong <sup>b,\*</sup>, Yi-Kuen LEE <sup>c</sup>,  
Wei-Zhen Lu <sup>a,\*</sup>

*a. Department of Architecture and Civil Engineering, City University of  
Hong Kong, Hong Kong SAR*

*b. Building Technology and Urban System Division, Lawrence Berkeley  
National Laboratory, Berkeley, CA 94720, USA*

*c. Department of Mechanical and Aerospace Engineering, The Hong Kong  
University of Science and Technology, Hong Kong SAR*

\* Corresponding authors:

E-mail address: [thong@lbl.gov](mailto:thong@lbl.gov); [bcwzlu@cityu.edu.hk](mailto:bcwzlu@cityu.edu.hk)

## **Abstract**

Large open spaces are popular nowadays in office buildings. However, occupants often complain too cold and/or too warm in large open spaces. It remains a challenge to control the operation of air-conditioning systems to provide occupant comfort in a large open space due to the ununiform distribution of internal heat gains and occupancy. Previous studies using CFD tools or building energy modelling tools alone did not solve the combined problem of the distributive temperature field in the space and the cooling demand from multiple terminal units. This study proposed to divide the large space into multiple subzone areas based on the layout of the terminal cooling equipment and the distribution of internal heat gains and occupancy. Then a coupling of FLUENT simulation with EnergyPlus building energy simulation is used to compute the optimal thermostat setpoint for each subzone to ensure uniform occupant comfort in the large space. EnergyPlus computes the interior wall surface temperatures and terminal unit supply air flowrate of each subzone, which are passed to the CFD simulations as boundary conditions; while FLUENT computes the temperature and PMV field, as well as airflow rates across the virtual partition walls between two adjacent subzones, which are passed to EnergyPlus for consideration as inter-zone air flow. A case study using an open office space in Hong Kong is conducted to demonstrate the validity of the methodology. Different temperature setpoints were computed for the subzones that achieved uniform occupant thermal comfort while

reducing energy use due to avoiding overcooling of the occupied surrounding. The results indicated that the coupling method can effectively provide a thermally comfortable environment with less energy use in large open office served by multiple terminal units.

**Keywords:** CFD Simulations; Building Energy Modelling; Thermal Comfort; Energy Performance

## **1. Introduction**

The building sector accounts for 40% of primary energy use, and a considerable fraction of building energy is utilized to construct a desirable indoor environment for occupants [1, 2, 3]. At the same time, people spend more than 90% of their time indoors with higher requirements of indoor thermal environment and thermal comfort [4,5]. Hence, the consistent improvement of building energy efficiency and better thermal comfort have become major concerns for the design and operation of heating, ventilation and air conditioning (HVAC) systems. Nowadays, modern open plan office becomes more popular than individual office rooms for better communication and money-saving. New challenges occur for the design and operation of HVAC systems in the large-space office due to high occupant density and complicated airflow and thermal operation management of multiple terminal units [6]. In modern open office spaces, the phenomena of overcooling and/or undercooling are common, which leads to the discomfort of workers as well as unnecessary waste of energy. Due to the trade-off between thermal comfort and energy saving, the standalone optimization of thermal comfort or energy performance cannot achieve these two goals concurrently. The coupling investigation of thermal comfort and energy performance of HVAC systems is proposed to provide a thermally comfortable indoor environment while consuming less energy in open office spaces.

To reduce building energy consumption, building energy modelling (BEM) programs have been widely used to optimize the energy

performance of lighting and HVAC systems [7]. As for the investigation of thermal comfort, CFD simulation is a powerful tool to estimate airflow patterns and thermal environment [8, 9]. In general, BEM and CFD simulations are independently adopted to optimize the energy performance and indoor environment of HVAC systems.

### 1.1 Comparisons between BEM and CFD simulations

These two simulation programs are distinct in the principle, computing time and applications [10, 11]. The principle of BEM programs like EnergyPlus is based on the nodal model by treating the building component as a node with homogenous characteristics, such as a unique temperature, pressure and concentration [5, 12]. The principle of BEM programs enable them with a short computing time to predict the energy performance of the building with multiple zones during a long period (e.g., one year / 8760 hours). However, the well-mixed room level air properties assumption of BEM makes it difficult to be applied to spaces with a non-uniform thermal environment.

Different from BEM programs, CFD simulation is capable to provide detailed representation of the thermal performance and indoor airflow patterns. The solution principle of CFD simulation is to discretize Navier-Stokes equations based on the finite volume method (FVM) by decomposing the room volume into numerous small control elements [19]. Besides the prediction of thermal parameters, CFD simulation can capture the properties of indoor airflow patterns using proper turbulence models. Such a principle makes a complete CFD simulation require intensive computing time and capacities. The differences between BEM and CFD simulations are summarized in Table 1.

Table 1 Comparison of features of BEM and CFD programs

	BEM (e.g., EnergyPlus)	CFD (e.g., Fluent)
Purpose	Energy / system sizing / control	Airflow/temperature/ comfort
Spatial resolution	Building / well-mixed zones	A single room/zone
Temporal	Annual 8760 hours at 5 to	1 day at seconds time

resolution	15 minutes time step	step
Challenge	Non-uniform space, airflow between zones and subzones	Intensive computing time, sensitive to boundaries
Weather data	Usually annual hourly weather data are available	Not included
Computing cost	Low	High

## 1.2 Applications of BEM-CFD simulation integration

Concerning the features of two simulation programs, researchers integrated two programs through manual or automated coupling methods to solve the challenges of each program. For example, the coupling of ESP-r and Fluent was applied to investigate the performance of a natural ventilation system, which shows that the coupling method can give accurate and effective predictions rather than the standalone program [13,14]. Zhai et al. explained the potentials to combine building energy modelling and CFD simulation, and the possible coupling approaches of two programs were explored [15]. In [3,16], the coupling strategies were applied to a heating office and an indoor auto-racing, which demonstrated that the coupling can improve the accuracy of the heating/cooling prediction. Zhang et al. integrated EnergyPlus with CFD simulation for a large-scale building with coupling variables of heat transfer coefficients, airflow rates and average air temperature [17]. The significant discrepancy for airflow simulation was identified between the nodal model and the coupled CFD-EnergyPlus model. Yamamoto et al. combined the energy simulation program with CFD simulation to detect the temperature distribution in a large space with floor heating system, which shows that the bulk temperature matches the energy simulation and CFD values by the combined approach [18]. In addition, the coupling method has been used to investigate the displacement ventilation (DV) systems. Due to the non-uniform temperature in the vertical dimension of DV systems, the standalone nodal model cannot give accurate predictions of the bulk temperature based on the assumption of air node with uniform properties.

The evaluation of the indoor environment of DV systems needs the aid of CFD simulations to provide spatial information on environmental parameters. Gowreesunker et al. coupled TRNSYS with CFD simulation to evaluate the performance of a displacement conditioning system [19], where TRNSYS was used for the control of the system with the airflow data provided by CFD simulation.

### **1.3 Research work contributions**

Based on the overview of applications of BEM-CFD simulation integration, the coupling method is able to investigate the thermal environment and energy performance concurrently. However, the applications mainly focus on natural ventilation systems and the space with the stratified thermal environment to address the vertical temperature non-uniformity. The implementation of the indoor environment with horizontal nonuniformity is rarely developed, particularly in large open spaces, where the horizontal non-uniform temperature distribution is always detected at the occupied level [20, 21]. To optimize thermal comfort in a large-space office, this study applies the integration of BEM and CFD simulation to explore optimal operation mode of the air conditioning system. The flowchart of the optimization process is shown in Fig. 1. The large-space office is divided into four subzones based on the initial temperature distributions and layout of fan coil units (FCUs). Three scenarios with different temperature setpoints are analysed by the coupling of BEM and CFD simulations. The BEM program estimates interior surface wall temperature and airflow rates of FCU for each subzone, which is passed to CFD simulation as boundary conditions. CFD simulations compute the airflow patterns, air temperature and PMV field in the space as well as the mass exchange rates between two adjacent subzones. The mass exchange rates are passed to the BEM program for the optimization of cooling energy of the air conditioning system.

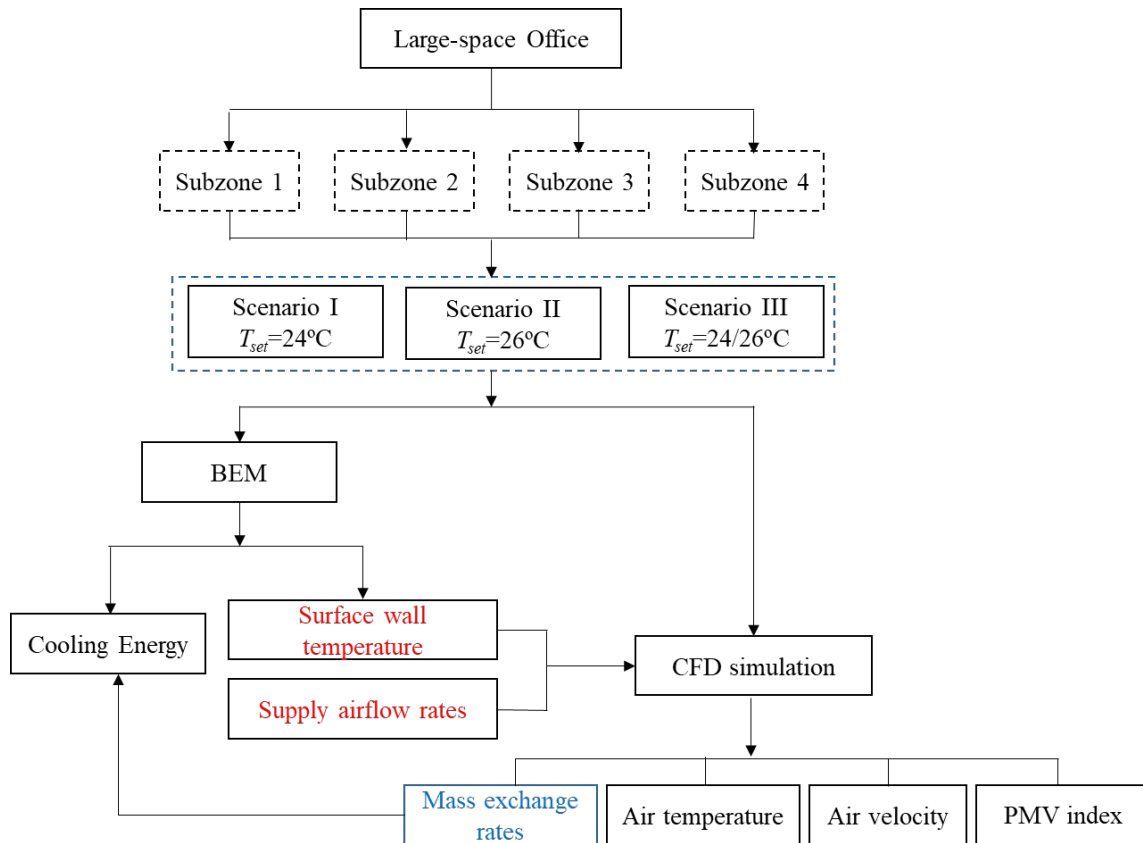


Fig. 1 The flowchart of the optimization process of thermal comfort

## 2. Methodology

### 2.1 Description of EnergyPlus and Fluent

As a integrate building and HVAC simulation tool, EnergyPlus is a widespread and accepted tool for building energy modelling [22]. The program simulates thermal conditions of buildings, the energy performance of systems and plants by considering the surface heat balance, air heat balance and building systems simulation with variable time steps and user-configurable modular system components [23]. The surface heat balance involves the heat conduction, convection and radiation occurring on the inside and outside surface of buildings [24]. While the air heat and mass balance deal with the mass streams, i.e., the ventilation air, exhaust air and infiltration air. Hence, EnergyPlus is capable to provide surface wall temperature, indoor air temperature, humidity, and radiant temperature, which can be set as the boundary conditions for CFD simulation. In addition, EnergyPlus program is able to perform the sizing calculation of HVAC systems, which can determine the



supply airflow rates, supply air temperature, and chilled water flow rates etc.

As for CFD simulation, there are many commercial and open-source tools, such as ANSYS Fluent, Open Foam, PHONETIC, CONTAM. As a commercial program, FLUENT is a powerful tool to simulate many fluid dynamics problems [25]. The principle is to solve Navier-Stokes (N-S) equations with appropriate turbulent models. The N-S equations consist of the conservation equations of mass, momentum and energy to describes the properties of fluid flow. There are typical turbulence models within the software, i.e., standard  $k-\varepsilon$  turbulent model, RNG  $k-\varepsilon$  turbulent model, large eddy simulation model. The program utilizes the finite volume method to solve N-S equations, which implies that the fluid domain is decomposed to many small control volumes. Based on the generated grid, the partial differential equations can be discretized into algebraic equations at each point of the grid. The calculation is conducted by means of iterating of these algebraic equations until the residuals meet the criteria. After the convergence of the calculation, the spatial profiles of the thermal environment and airflow patterns can be obtained.

## **2.2 Coupling framework of BEM and CFD programs**

Two coupling strategies of BEM and CFD simulation are available: internal coupling and external coupling. Internal coupling requires two programs sharing the same server, while external coupling signifies that two programs run on two separate servers. Considering the discontinuities of two programs in time scale, computing time and speed, the external coupling is more robust and easier to converge compared with the internal coupling [26, 27]. Hence, in this study, the external coupling with two-way data synchronization method is adopted. The EnergyPlus program considers the air flow features estimated by FLUENT, and reliable boundary conditions of numerical simulations are provided by EnergyPlus program. The coupling framework of EnergyPlus and FLUENT is demonstrated in Fig. 2. As shown in Fig. 2, EnergyPlus has been first generated the surface temperature and supply airflow rates for FLUENT.

With the supplied boundary conditions from EnergyPlus, CFD simulation with FLUENT is conducted to obtain the spatial distributions of temperature and air speed inside the large open office. Based on the profiles of environmental parameters, thermal comfort is further evaluated based on the thermal comfort model. In addition to the thermal environment, CFD simulation predicts detailed airflow patterns inside the large space. With respect to air flow parameters, EnergyPlus is re-run considering the zone mixing in the space to estimate the energy consumptions of HVAC systems. Therefore, under such a coupling framework, the simultaneous optimization of the indoor environment, as well as energy performance of air conditioning systems can be achieved.

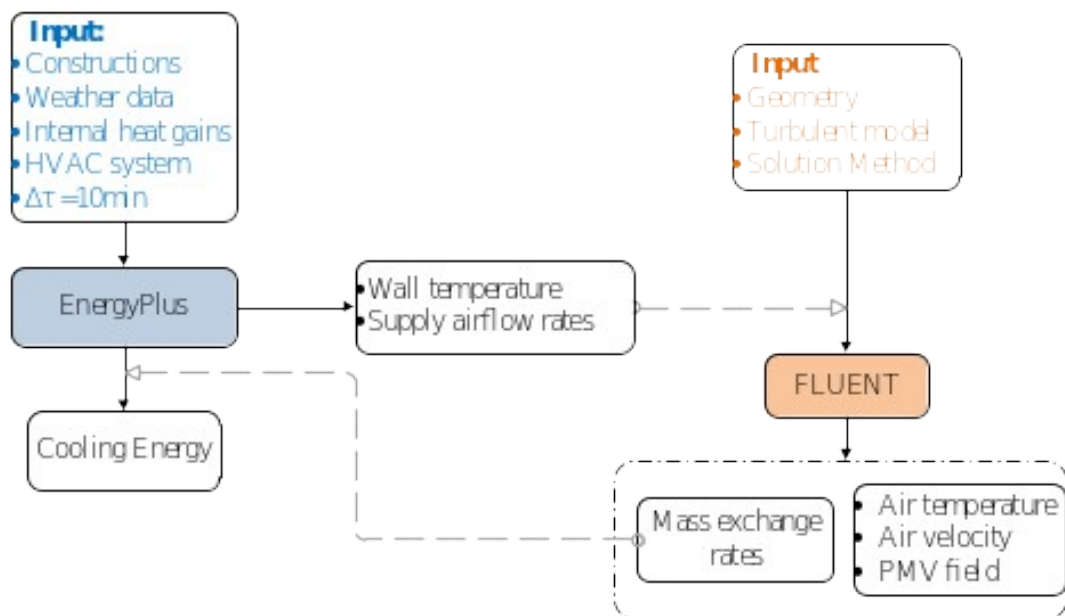


Fig. 2 The coupling approach of EnergyPlus and Fluent program

### 2.3 Thermal comfort metrics

The thermal comfort model used in this study is predicted mean votes and predicted percentage dissatisfied (PMV-PPD) model proposed by Fanger [28]. The PMV-PPD thermal comfort model evaluates the thermal sensations of occupants with 7 levels ranging from -3 to +3 corresponding to the thermal sensations of cold, cool, slightly cool, neutral, slightly warm, warm and hot. The PMV values depend on six influence factors including environmental parameters and human factors. Four environmental parameters consist of air temperature, air speed, relative

humidity and mean radiant temperature. While two human factors are the metabolic rates and clothing insulations.

In this study, the spatial distributions of the PMV index in a large office are estimated by the CFD simulation, which can offer useful diagnostics for occupants' discomfort. Moreover, the optimisation of thermal comfort is achieved through the co-simulation of EnergyPlus and FLUENT according to the spatial profiles of the PMV index.

### **3. Simulation case study**

#### **3.1 The description of the large open office**

The test large office is located at Hong Kong with the dimension of 11.5m in length, 10.5m in width and 2.4m in height. The office has an east-orientation external wall, and the west wall is adjacent to a corridor with an internal window. Other walls are internal walls adjacent to air-conditioned space. Inside the large office, 36 workstations are distributed in 6 columns. Each workstation has one subject equipped with a computer and a display. In addition, 27 lamps are deployed at the ceiling level. As for the air conditioning system in the large office, four fan coil units (FCU) are implemented to supply cold air to offset internal heat gains and keep the room air temperature at a comfortable level. Coupled with the cooling system, the ventilation plan is attained by two fresh air inlets in the middle area to supply the proper amount of fresh air to maintain the concentrations of carbon-oxygen at an acceptable level. The layout scheme of the large office is shown as Fig. 3.

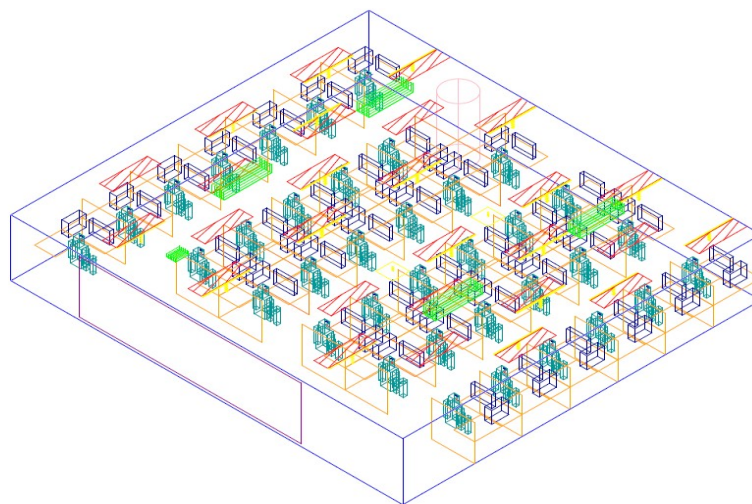
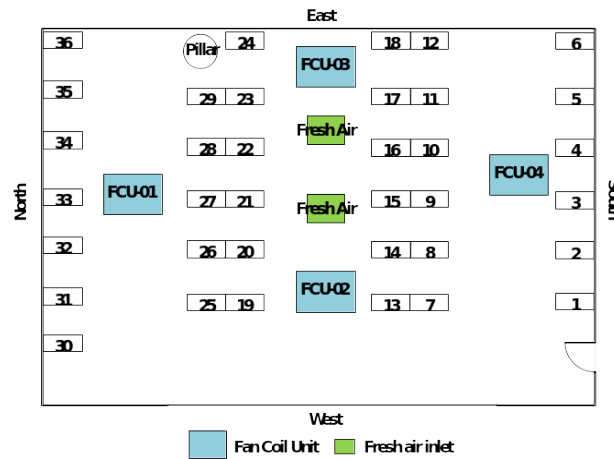


Fig. 3 The layout scheme of the large open office in the bird's eye and 3D view

### 3.2 Non-uniform temperature distributions in the large open office

Based on the initial CFD simulations of the large office, non-uniform temperature distributions are detected under the temperature setpoint of 23°C. Fig. 4 illustrates the temperature distributions at Plane Y = 1.2 m corresponding to the seating head level. It can be found that the lowest temperature value is around 23°C in the middle area, while the highest temperature value is 26°C in the side areas. The maximum temperature differences reach 3°C in the occupied plane. The non-uniform thermal environment may further lead to occupants' discomfort as occupants in the middle areas feeling cool while occupants at side areas feeling warm, and hence the non-uniformity of the thermal comfort exists in the large

space office.

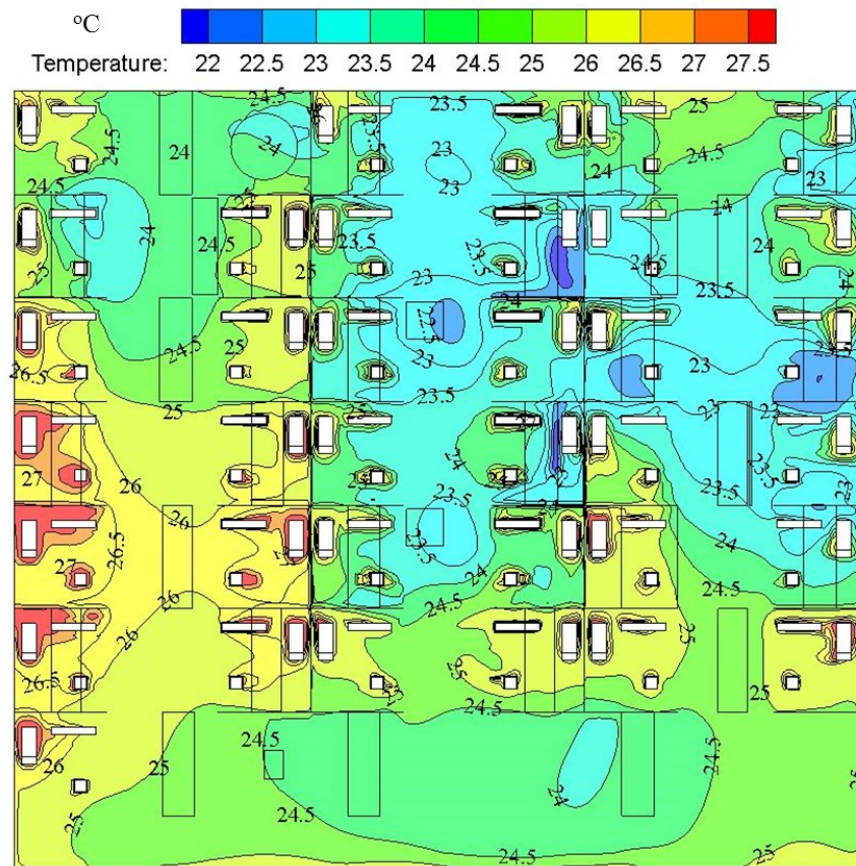


Fig. 4 Temperature distributions at occupied plane  $Y = 1.2$  m

In order to settle the non-uniformity of indoor air temperature, the large office is divided into four subzones according to the spatial distributions temperature and the layout scheme of FCUs, as shown in Fig. 5. Subzones 1 and 4 correspond the side areas with FCU-01 and FCU-04 respectively, and Subzones 2 and 3 are located at the middle of the space equipped with FCU-02 and FCU-03 respectively. With respect to the division scheme, different temperature setpoints are attributed to each subzone as depicted in Fig. 5. Scenario I and II represent the homogenous temperature setpoint at four subareas, while multiple setpoints of subzones are set in Scenario III. In order to achieve the uniform temperature distribution of the large space office, the co-simulation between EnergyPlus and FLUENT is performed under three scenarios.

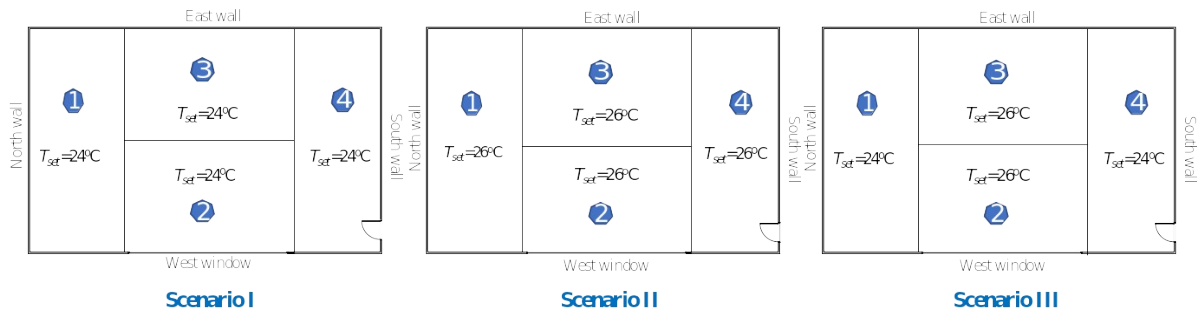


Fig. 5 The demonstration of temperature setpoints of three scenarios

### 3.3 EnergyPlus modelling

In order to obtain the surface temperature and supply airflow rates, the EnergyPlus modelling for the large open office is first performed. The IDF file mainly includes the information of constructions, the internal loads and HVAC systems. As demonstrated in Fig. 6, the definition of subzones and surface wall is clarified. As the large open office is adjacent to a corridor with a curtain glass wall shown as Z5\_west\_win, zone 5 was added to represent the corridor to investigate the effect of solar radiation on the internal window surface temperature on the west wall of the large office.

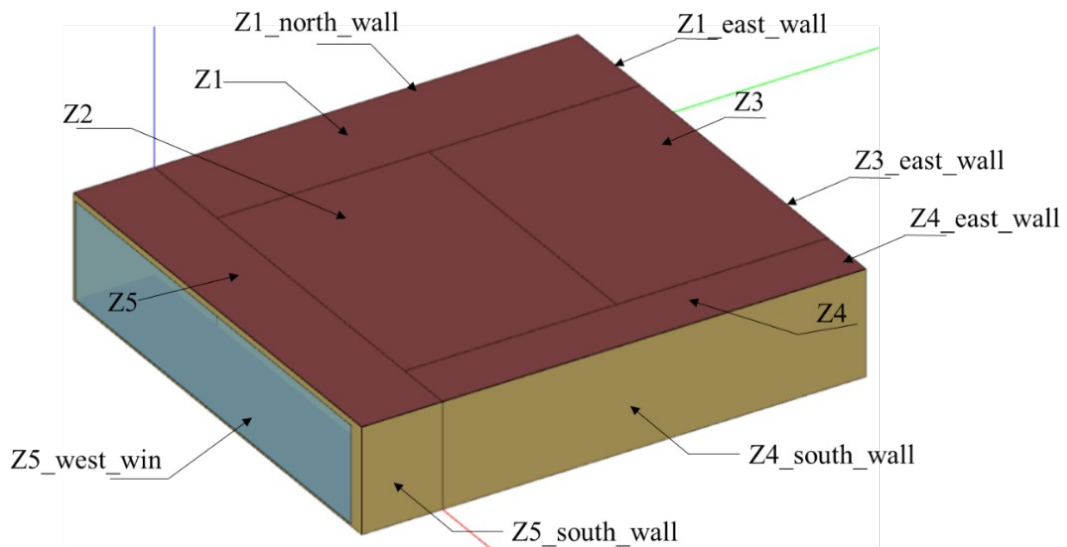


Fig. 6 The subzones and surface definition in EnergyPlus modelling

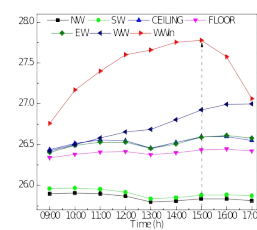
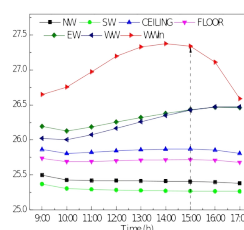
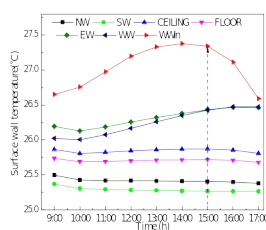
In addition, the detailed settings of the EnergyPlus model are summarized in Table 2. The heat power of occupants, lamps and electric devices are 70W, 40W, 100W respectively, which is in consistent with the thermal boundary conditions of these items in Fluent program. The EnergyPlus modelling is performed during a typical summer day in Hong

Kong from 9:00 to 17:00 to predict the surface wall temperature and supply airflow rates under different temperature setpoints.

Table 2 Settings of EnergyPlus model in the large open office

Type	Subzone1	Subzone 2	Subzone 3	Subzone 4
Dimension	2.5m×10.	7.5m×5.3m	7.5m×5.2m	1.5m×10.
Occupants	7×70W	12×70W	11×70W	6×70W
Lamps	7×40W	8×40W	6×40W	6×40W
Electric equipment	7×100W	12×100W	11×100W	6×100W
HVAC system	FCU	FCU	FCU	FCU
Ventilation system	NA	Fresh air	Fresh air	NA
		0.085m <sup>3</sup> /s	0.085m <sup>3</sup> /s	

The changing patterns of interior surface wall temperature are predicted by EnergyPlus simulation under three scenarios, as shown in Fig. 7. According to the figure, the surface temperature of the internal walls is stable, i.e., the north wall, the south wall, the ceiling and the floor, while that of external walls varies throughout the day. Taking Scenario I as an example, because of the influence of solar radiation on the external wall, the surface temperature of the east wall presents a slightly increasing from 10:00 and reaches a peak at 15:00 with the value of 26.4°C. As the west wall is adjacent to a corridor with a curtain glass wall, the surface temperature of the west wall possesses a similar trend to the east wall. The surface temperature of the west window is higher than the wall temperature due to the solar radiation heat transfer. The whole changing pattern of the window temperature seems like a bell with a peak value around 15:00. The coupled simulation between EnergyPlus and Fluent is conducted under the peak load condition.



(a) Scenario I  
Scenario III

(b) Scenario II

(c)

Fig. 7 Interior surface temperature of the large open office

Besides the interior surface temperature, the design supply airflow rates of the HVAC system under three scenarios are also estimated by EnergyPlus modelling. As listed in Table 3, the air change rates of each subzone under three scenarios are resolved. Due to the lowest temperature setpoint under Scenario I (24°C), the supply airflow rates are the largest compared to the other two scenarios. These supply airflow rates are set as the boundary conditions for CFD simulations.

Table 3 The supply airflow rates of FCU

Zone Name	Scenario I ACH (h <sup>-1</sup> )	Scenario II ACH (h <sup>-1</sup> )	Scenario III ACH (h <sup>-1</sup> )
Thermal Zone 1	9	6.9	9
Thermal Zone 2	10.7	8.2	8.2
Thermal Zone 3	8.9	6.5	6.5
Thermal Zone 4	12.5	9.6	12.5

### 3.4 CFD modelling

#### 3.4.1 Meshing scheme of the large open office

Prior to the CFD simulation, proper meshing scheme is supposed to be generated as the fundamental PDEs need to be discretized into algebraic equations at each grid point. Generally, there is a balance between computing time and accuracy in terms of meshing schemes. Too coarse meshing cannot provide accurate simulation results of airflow patterns and thermal conditions. Too fine meshing could give accurate simulation results yet require much more computing time and capacities. In order to solve the trade-off between two issues, a hexa-structured mesh scheme is generated within the large office with about 3 million hexahedral elements. In order to capture the airflow properties around complicated geometry, the mesh is refined at the supply inlet areas and the areas



around internal heat sources, i.e., occupants, computers and lamps. As shown in Fig. 8, the meshing scheme at Plane Y = 1.2 m are illustrated.

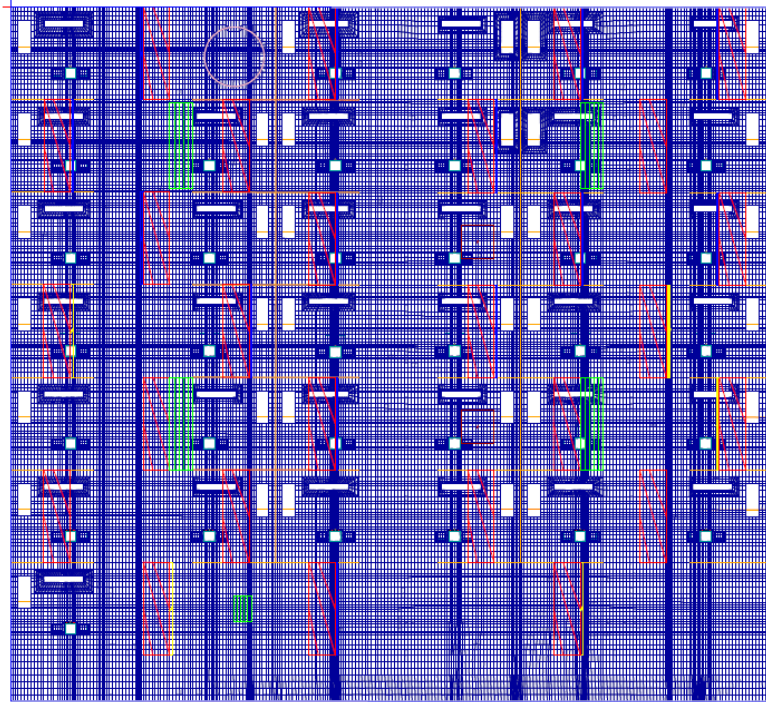


Fig. 8 The meshing scheme at Plane Y = 1.2 m

### 3.4.2 Numerical process

Considering the conservation equations of mass, momentum and energy, the time-averaged equations for the incompressible flow can be expressed in a general form including four items: transient item, convection item, diffusion item and source item, expressed as Eq. (1):

$$\frac{\partial(\rho\phi)}{\partial t} + \text{div}(\rho\phi\vec{u}) = \text{div}(\Gamma\text{grad}\phi) + S_\phi$$

Transient    Convection    Diffusion    Source

(1)

where  $\phi$  denotes the dependent variable, which may stand for velocity component  $u_i$  in  $i$  dimension, temperature  $T$ ;  $t$  is the time,  $\vec{u}$  is the velocity vector,  $\Gamma$  means the diffusion coefficient, and  $S_\phi$  is the source term.

The solution of N-S equations requires the assist of turbulent models. Concerning the indoor airflow, there are typically three kinds of fluid types: laminar airflow, turbulent airflow with standard  $k-\varepsilon$  model and turbulent airflow with RNG  $k-\varepsilon$  model. According to the comparison of different indoor turbulent models [29, 30, 31], RNG  $k-\varepsilon$  turbulent model presents the best performance to predict the indoor airflow properties as

the turbulent model can be not only applied to low-speed indoor airflow, but also to airflow with high speed. RNG  $k$ - $\varepsilon$  turbulent model adopts the renormalization group methods to derive the constant values related to turbulent kinetic energy,  $k$  and its rate of dissipation  $\varepsilon$  [32]. In this study, the RNG  $k$ - $\varepsilon$  turbulent model is used to predict the indoor airflow patterns of the large space office. Coupled with the imposed boundary conditions, the solution for finite difference equations is through an iterative procedure that implements the Line Gauss-Seidel method and the SIMPLE algorithm [33]. The residual criterion of convergence for continuity, momentum, turbulent kinetic energy and turbulent dissipation rate is  $10^{-3}$ , and for energy is  $10^{-6}$ . The numerical simulation is carried out on a cluster with 40 CPU. A complete simulation basically requires 1h for each case.

### 3.4.3 Boundary conditions

Apart from the meshing generation, the boundary condition is another vital part for CFD simulations as different settings of boundary conditions will lead to completely distinct results. As described in previous EnergyPlus modelling, the setting of boundary conditions in CFD simulations consists of the internal loads, the supply air inlet, the return air vent, and the enclosure. The detailed configuration of the boundary conditions is summarized in Table 4. The thermal conditions of internal loads are set as the constant heat flux equal to the heat generation power in EnergyPlus model. The supply air inlet is the velocity inlet with a constant supply air temperature of 16°C, and the return air vent is pressure outlet. The thermal conditions for the enclosure are consistent with the internal surface temperature predicted by EnergyPlus model under the peak load condition.

Table 4 The setting of boundary conditions in the large open office

Name	Dimension	Boundary conditions
Office	11.5m×10.5m×2.4m	Fluid domain
Supply air inlet	1.4m×0.04m	Velocity inlet, $T_s=16^\circ\text{C}$
Fresh air inlet	0.5m×0.5m	Velocity inlet, $T_s=16^\circ\text{C}$

Return air vent	1.4m×0.35m	Pressure outlet
Occupants	0.4m×0.2m×1.2m	Heat flux rate: 44W/m <sup>2</sup>
Computers	0.2m×0.5m×0.5m	Heat flux rate: 67W/m <sup>2</sup>
Monitor	0.5m×0.1m×0.5m	Heat flux rate: 57W/m <sup>2</sup>
Lamps	1.4m×0.4m	Heat flux rate: 71W/m <sup>2</sup>
Walls	the same as EnergyPlus model	Surface temperature

---

## 4. Results and Discussion

### 4.1 Temperature and PMV values of subzones at occupied area

#### 4.1.1 Mean air temperature and PMV values at occupied area

Based on the co-simulation of EnergyPlus and Fluent, the spatial distributions of environmental parameters can be estimated, and thus the mean air temperature and PMV values at occupied zone under three scenarios are solved as shown in Fig. 9. It can be found that there are discrepancies between the temperature setpoints and the mean air temperature in the occupied area. As for Scenario I, the predicted mean air temperature ranges from 22.5°C to 23.5°C while the setpoint temperature for this scenario is 24°C, which signifies that a maximum temperature difference of 1.5°C is detected by the co-simulation between EnergyPlus and CFD modelling. Besides such discrepancies, the temperature differences among four subzones are found indicating that the non-uniformity of temperature exists in the large open office. Generally, subzone 3 possesses the lowest mean air temperature, subzone 2 follows and subzones 1&4 have a higher air temperature yet still below the setpoints. Such distributions are owing to the extra fresh air inlets at subzones 2&3 with the same supply air temperature as the air conditioning systems. When comparing Scenario I & II to Scenario III, the relatively uniform temperature is achieved under Scenario III with multiple setpoints for the temperature differences are with 0.5°C among subareas.

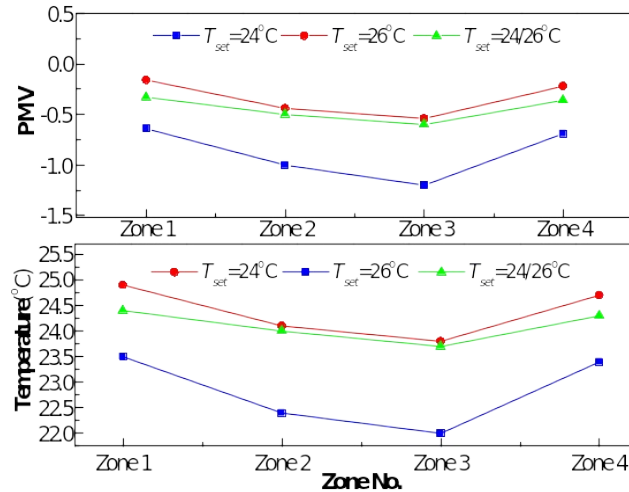


Fig. 9 Temperature and PMV values at the occupied area under three scenarios

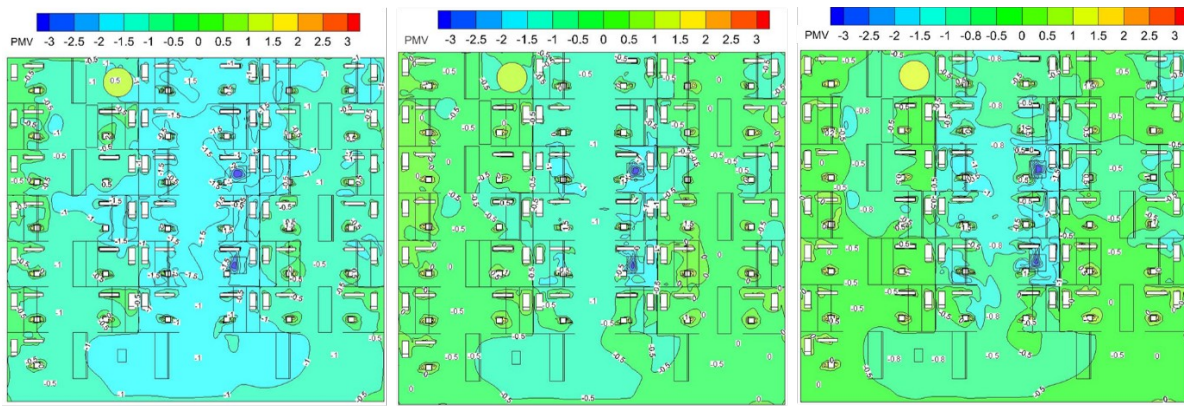
Fig. 9 also presents the PMV values at the occupied area of three scenarios agreeing with the trends of air temperature due to the indoor environment with low air speed is a relatively stable environment, and the temperature mostly affects the thermal sensations of occupants. Except for the patterns of PMV values, the specific values of PMV metric mean occupants under three scenarios feel cool as all PMV values are below 0. When the temperature setpoint is 24°C, the PMV values are in the scope of -1.2 to -0.5. With the temperature setpoint of 26°C, the PMV values at the occupied zone are the highest ranging from -0.4 to -0.1 complying with ASHRAE thermal comfort standard. While under scenario III, the variation of PMV values within four subzones is the smallest with following the standards as the values range from -0.5 to -0.3. Therefore, the separate temperature setpoints present potentials to achieve uniform thermal comfort compared to the single setpoint in terms of the distributions of air temperature and PMV values.

#### 4.1.2 Distributions of PMV values at occupied area

To investigate the thermal conditions around occupants, the PMV values are solved based on PMV-PPD thermal comfort model. In terms of

environmental parameters, CFD simulations predict the spatial profiles of air temperature and air speed inside the large office. The relative humidity is assumed as 65%, and mean radiant temperature is exported from EnergyPlus modelling. As for the two human factors, the metabolic rates of seated occupants in the office is 70W with the clothing insulation of 0.8 clo according to the thermal comfort standard. With the all necessary data, the UDF file is interpreted in Fluent program to calculate the spatial distributions of thermal comfort metric.

The spatial distributions of PMV values at Plane  $Y = 1.2$  m under three scenarios are presented in Fig. 10. Plane  $Y = 1.2$  m corresponds to the head level for the seated occupants in the office. The PMV values under Scenario I in most areas are below -0.5, which signifies the occupants may feel cold when the temperature setpoint is 24°C. The middle areas including subzones 2&3 are colder than the other two subzones as the PMV values in these areas range between -1.5 and -1. As for the side areas, the PMV values are between -0.5 to -1, which indicates that occupants at side areas feel a little warmer than occupants in the middle area. As for Scenario II, the temperature setpoint is 26°C. Compared with Scenario I, the range of PMV values of this scenario is from -0.5 to -1 in middle areas while the PMV values are between 0 and -0.5 at side areas which are within the thermal comfort zone. Different from the homogenous setpoints, the temperature setpoints in Scenario III are separate in the subzones. The PMV values at Plane  $Y=1.2$ m under such a setting are more uniform than homogenous temperature setpoints as all the PMV values are around -0.5. Therefore, the multiple temperature setpoints based on the zones can attain the uniform thermal environment in the large open office.



PMV contour at Y=1.2m  
Scenario I:  $t_{set}=24^{\circ}\text{C}$

PMV contour at Y=1.2m  
Scenario II:  $t_{set}=26^{\circ}\text{C}$

PMV contour at Y=1.2m  
Scenario III:  $t_{set}=24/26^{\circ}\text{C}$

Fig. 10 Spatial distributions of PMV values at occupied area

## 4.2 Mass flow rates between adjacent subzones

Because the CFD simulations can conduct intensive calculations of airflow characteristics, the mass exchange rates between two interactive subzones are obtained. The calculation of the mass flow rates is on the basis of flow filed in the office. The mass flow rates on the virtual plane of two adjacent subzones can be resolved by CFD simulation.

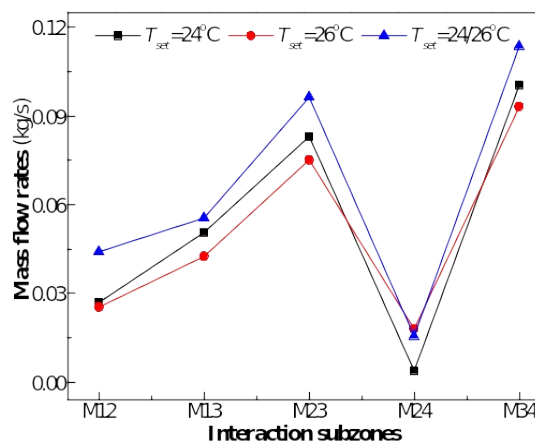


Fig. 11 The mass exchange rates between interaction subzones

Fig. 11 shows the mass flow rates between two interactive subzones  $M_{ij}$  under three scenarios, where  $M_{ij}$  denotes the mass flow rates are transferred from subzone  $i$  to subzone  $j$ . Based on the figure, it can be found that the mass flow rates between adjacent two subzones under

multiple temperature setpoints are larger than the homogenous temperature setpoint. Such phenomena may be due to the temperature differences accelerating the mass exchanging. The changing patterns of mass flow rates between interactive subzones under three scenarios are similar, and the mass flow rates between subzone 3 and 4 are the largest while between subzone 2 and 4 are the lowest.

#### **4.3 Return air temperature estimated by CFD simulation**

In principle, the room air temperature in EnergyPlus model is equal to the return air temperature of HVAC systems according to the well mixed-mode assumption. However, the return air temperature cannot agree with the assumption in real practice. The air temperature at return vents is exported by CFD simulation program to figure out the discrepancies of return air temperature between the real and ideal conditions. As shown in Fig. 12, the return air temperature of four return vents is presented through the coupling of EnergyPlus and CFD simulations. The room and return air temperature should be 24°C under Scenario I, but the actual return air temperature is 1°C lower compared with the temperature setpoint. Similar results are discovered in Scenario II, the return air temperature is 24.5°C while the temperature setpoint is 26°C. Different from the single setpoint, separate temperature setpoints are adopted in Scenario III as the setpoint for subzones 1 and 4 is 24°C and for subzones 2 and 3 is 26°C. But the results show that the return air temperature predicted by the co-simulation is 24°C for subzones 2 and 3 and 24.7°C for subzones 1 and 4. Therefore, the return temperature predicted by CFD simulation is lower than the temperature setpoints as a result of the well-mixed assumptions of EnergyPlus. Because under such an assumption, EnergyPlus program risks overestimating the cooling loads of air conditioning systems.

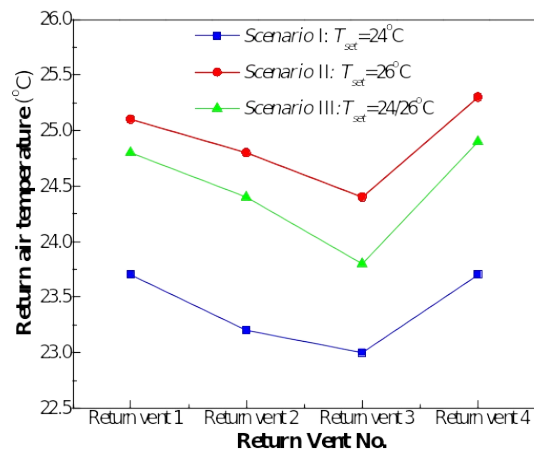


Fig. 12 Return air temperature predicted by the co-simulation

#### 4.4 Cooling energy consumptions under three scenarios

As predicted mass exchange rates by Fluent are exported to EnergyPlus model, the cooling energy is recalculated in EnergyPlus program. The mass exchange rates between two adjacent subzones are set in EnergyPlus program with the zone mixing model to consider the airflow parameters. Fig. 13 shows the comparisons of cooling energy consumptions with and without zone mixing. For the homogenous temperature setpoint, the cooling energy considering zone mixing is lower than the standalone model. The cooling energy presents a potential of 3.5% energy saving by means of the integration of EnergyPlus and Fluent programs. The results also imply that the standalone EnergyPlus model may overestimate the cooling loads of the HVAC system without considering the zone mixing in the large open office. However, under the scenario of separate temperature setpoints, the cooling energy is almost the same with and without considering the zone mixing, which indicates the non-uniformity of temperature normally exists in the large open office, while the assumption of homogenous temperature leads to the prediction of cooling energy deviating the real condition.



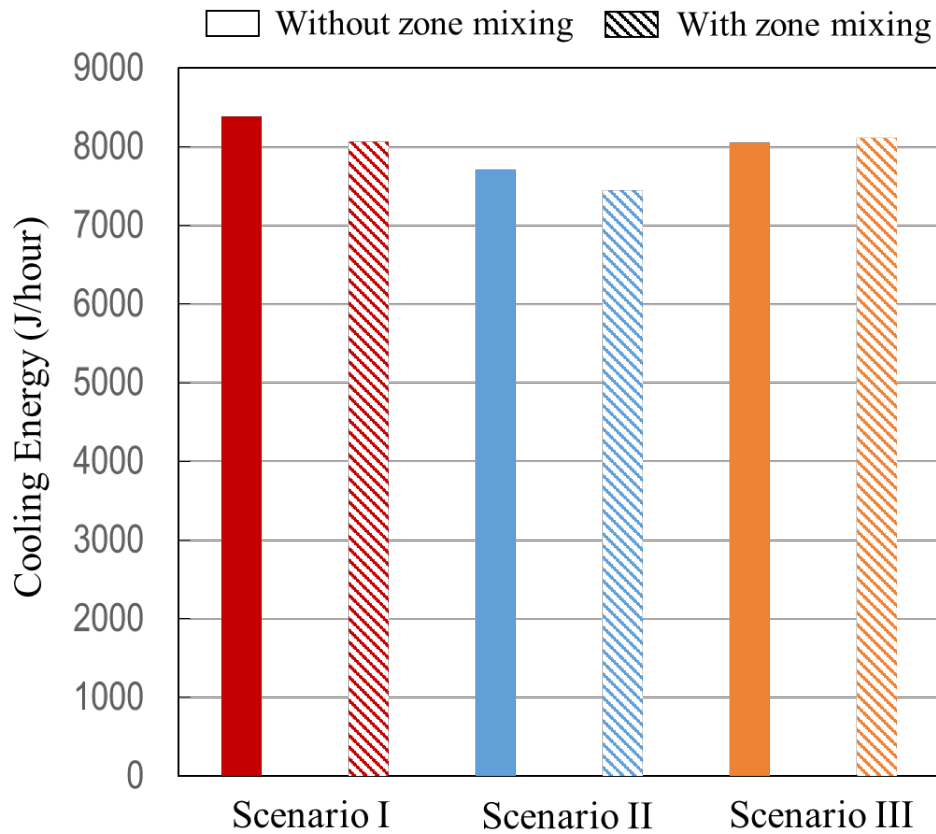


Fig. 13 Comparisons of cooling energy consumptions between with/without zone mixing

## 5. Discussion

In views of nonuniform thermal environment in large open spaces, the proposed coupled BEM and CFD simulation framework can be used to evaluate and guide the operation of multiple terminal units to attain uniform spatial thermal comfort. Based on the co-simulation results of three scenarios, the subzone thermostat control is more applicable than the traditional single thermostat control with consideration of the non-uniform distributions of occupants and internal heat gains in the large office. The optimal operation of multiple terminal units in the large office should focus on the subzones rather than the entire space. Furthermore, the division scheme of subzones needs to consider the spatial distributions of internal heat sources as well as the layout of terminal units, e.g., fan coil units, air conditioners. The supply air volume of terminal units for each subzone should be determined based on the temperature setpoint of subzones. The multiple thermostat control of

subzones and individual supply air volume to each subzone generally can provide a uniform thermal comfort environment for occupants in the large open spaces.

## **6. Conclusions**

This study integrates the CFD simulation with building energy modelling to optimize the non-uniform thermal environment in a large open office. The steady two-way coupling is adopted with EnergyPlus model exporting surface wall temperature and subzone supply airflow rates to CFD program, and air mass exchange rates output from CFD simulation to EnergyPlus simulation. The PMV-PPD thermal comfort model is used to evaluate the thermal comfort of occupants. In order to achieve the uniform thermal comfort environment, the large open office is divided into four subzones based on the layout scheme of FCUs and previous temperature profiles of the large office. The co-simulation of EnergyPlus and Fluent is performed under three scenarios with different temperature setpoints to find the optimal setting of the HVAC system while achieving a uniform thermal environment. The key findings are summarized as follows:

- (1) Considering the outdoor conditions, EnergyPlus model passes accurate interior surface wall temperature and supply airflow rates to CFD simulation;
- (2) Through CFD simulation, the spatial distribution of PMV values is obtained. Based on the analysis of PMV values in the occupied area, multiple temperature setpoint for the different four subzones have more potentials to achieve uniform thermal environment than the single temperature setpoint for the entire space. With the temperature setpoint of 24°C for subzones 1&4 and 26°C for subzones 2&3, the PMV values at Plane Y = 1.2 m range from -0.5 to 0, complying with the ASHRAE 55 thermal comfort standard;
- (3) The discrepancies are detected between the return air temperature and the temperature set-point through the co-simulation. Based on the solution principle and the well-mixed air conditions assumption,

EnergyPlus model regards the return air temperature the same as temperature setpoint. In fact, the return air temperature predicted by CFD simulation is lower than the temperature setpoint, which signifies that the EnergyPlus model may overestimate the supply conditions. Under three scenarios, the discrepancies between the return air temperature and the temperature setpoint range from 1 to 1.5°C.

- (4) As CFD simulations conduct the intensive calculation of indoor airflow, the air exchange rates between two adjacent subzones are exported to EnergyPlus. Comparing the air exchange rates of three scenarios, the air exchange rates are the largest under Scenario III with separate temperature set-points for each subzone.
- (5) Concerning the air flow between subzones, the cooling energy consumptions are recalculated by EnergyPlus with the zone mixing module. Through the comparison of the cooling energy consumption with and without considering zone mixing, 3.5% cooling energy saving is found with the consideration of zone mixing in the large open office. This phenomenon also indicates that the standalone EnergyPlus model may risk overestimating the cooling energy and resulting in unnecessary cooling energy waste.

## **Acknowledgements**

The work was partially supported by Strategic Research Grant, City University of Hong Kong Grant (7004867), Innovation and Technology Fund (ITF) (ITS/410/16FP & CityU-9678142). Authors would like to thank the assistance provided from Facility Management Office, Hong Kong University of Science and Technology. This work is also supported by the Assistant Secretary for Energy Efficiency and Renewable Energy of the United States Department of Energy under Contract No. DE-AC02-05CH11231.

## References

- <sup>1</sup> Cehlin, M., Karimipannah, T., Larsson, U., & Ameen, A., 2019. Comparing thermal comfort and air quality performance of two active chilled beam systems in an open-plan office. *Journal of Building Engineering*, 22, 56-65.
- <sup>2</sup> Pérez-Lombard, L., Ortiz, J., & Pout, C., 2008. A review on buildings energy consumption information. *Energy and buildings*, 40(3), 394-398.
- <sup>3</sup> Poel, B., van Cruchten, G., & Balaras, C. A., 2007. Energy performance assessment of existing dwellings. *Energy and Buildings*, 39(4), 393-403.
- <sup>4</sup> Rupp, R. F., Vásquez, N. G., & Lamberts, R., 2015. A review of human thermal comfort in the built environment. *Energy and Buildings*, 105, 178-205.
- <sup>5</sup> Yang, L., Yan, H., & Lam, J. C., 2014. Thermal comfort and building energy consumption implications—a review. *Applied energy*, 115, 164-173.
- <sup>6</sup> Arghand, T., Karimipannah, T., Awbi, H. B., Cehlin, M., Larsson, U., & Linden, E., 2015. An experimental investigation of the flow and comfort parameters for under-floor, confluent jets and mixing ventilation systems in an open-plan office. *Building and Environment*, 92, 48-60.
- <sup>7</sup> Harish, V. S. K. V., & Kumar, A., 2016. A review on modeling and simulation of building energy systems. *Renewable and Sustainable Energy Reviews*, 56, 1272-1292.
- <sup>8</sup> Tsou, J. Y., 2001. Strategy on applying computational fluid dynamic for building performance evaluation. *Automation in Construction*, 10(3), 327-335.
- <sup>9</sup> Chen, Q., 2009. Ventilation performance prediction for buildings: A method overview and recent applications. *Building and environment*, 44(4), 848-858.
- <sup>10</sup> Fouquier, A., Robert, S., Suard, F., Stéphan, L., & Jay, A., 2013. State of the art in building modelling and energy performances prediction: A review. *Renewable and Sustainable Energy Reviews*, 23, 272-288.
- <sup>11</sup> Zhai, Z., Chen, Q., Klems, J. H., & Haves, P., 2001. Strategies for coupling energy simulation and computational fluid dynamics programs (No. LBNL-48286). Ernest Orlando Lawrence Berkeley National Laboratory, Berkeley, CA (US).
- <sup>12</sup> Axley, J., 2007. Multizone airflow modeling in buildings: History and theory. *HVAC&R Research*, 13(6), 907-928.
- <sup>13</sup> Wang, L. and Wong, N.H., 2008. Coupled simulations for naturally ventilated residential buildings. *Automation in Construction*, 17(4), 386-398.
- <sup>14</sup> Tan, G., & Glicksman, L. R., 2005. Application of integrating multi-zone model with CFD simulation to natural ventilation prediction. *Energy and Buildings*, 37(10), 1049-1057.
- <sup>15</sup> Zhai, Z., Chen, Q., Haves, P., & Klems, J. H., 2002. On approaches to couple energy simulation and computational fluid dynamics programs. *Building and Environment*, 37(8-9), 857-864.
- <sup>16</sup> Zhai, Z. J., & Chen, Q. Y., 2005. Performance of coupled building energy and CFD simulations. *Energy and buildings*, 37(4), 333-344.
- <sup>17</sup> Zhang, R., Lam, K. P., Yao, S. C., & Zhang, Y., 2013. Coupled EnergyPlus and computational fluid dynamics simulation for natural ventilation. *Building and Environment*, 68, 100-113.

- 18 Yamamoto, T., Ozaki, A., Lee, M., & Kusumoto, H., 2018. Fundamental study of coupling methods between energy simulation and CFD. *Energy and Buildings*, 159, 587-599.
- 19 Gowreesunker, B. L., Tassou, S. A., & Kolokotroni, M., 2013. Coupled TRNSYS-CFD simulations evaluating the performance of PCM plate heat exchangers in an airport terminal building displacement conditioning system. *Building and Environment*, 65, 132-145.
- 20 Zhou, P., Huang, G., & Li, Z., 2014. Demand-based temperature control of large-scale rooms aided by wireless sensor network: Energy saving potential analysis. *Energy and buildings*, 68, 532-540.
- 21 Zhou, P., Huang, G., Zhang, L., & Tsang, K. F., 2015. Wireless sensor network based monitoring system for a large-scale indoor space: data process and supply air allocation optimization. *Energy and Buildings*, 103, 365-374.
- 22 Fumo, N., Mago, P., & Luck, R. (2010). Methodology to estimate building energy consumption using EnergyPlus Benchmark Models. *Energy and Buildings*, 42(12), 2331-2337.
- 23 Crawley, D. B., Lawrie, L. K., Winkelmann, F. C., Buhl, W. F., Huang, Y. J., Pedersen, C. O. & Glazer, J., 2001. EnergyPlus: creating a new-generation building energy simulation program. *Energy and buildings*, 33(4), 319-331.
- 24 Strand, R., Buhl, F. W. F., Huang, J., & Taylor, R., 1999. Enhancing and extending the capabilities of the building heat balance simulation technique for use in EnergyPlus. In *in Proceedings of Building Simulation'99, Volume II*.
- 25 Fluent, A. N. S. Y. S., 2015. Theory guide. *Ansys Inc*.
- 26 Djunaedy, E., Hensen, J. L., & Loomans, M. G. L. C., 2003. Toward external coupling of building energy and airflow modeling programs. *ASHRAE Transactions*, 109(2), 771-787.
- 27 Tian, W., Han, X., Zuo, W., & Sohn, M. D., 2018. Building energy simulation coupled with CFD for indoor environment: A critical review and recent applications. *Energy and Buildings*, 165, 184-199.
- 28 Fanger, P. O., 1970. Thermal comfort. Analysis and applications in environmental engineering. *Thermal comfort. Analysis and applications in environmental engineering*.
- 29 Chen, Q., 1995. Comparison of different k- $\epsilon$  models for indoor air flow computations. *Numerical Heat Transfer, Part B Fundamentals*, 28(3), 353-369.
- 30 Zhai, Z. J., Zhang, Z., Zhang, W., & Chen, Q. Y., 2007. Evaluation of various turbulence models in predicting airflow and turbulence in enclosed environments by CFD: Part 1—Summary of prevalent turbulence models. *Hvac&R Research*, 13(6), 853-870.
- 31 Zhang, Z., Zhang, W., Zhai, Z. J., & Chen, Q. Y. (2007). Evaluation of various turbulence models in predicting airflow and turbulence in enclosed environments by CFD: Part 2—Comparison with experimental data from literature. *Hvac&R Research*, 13(6), 871-886.
- 32 Shan, X., Xu, W., Lee, Y. K., & Lu, W. Z., 2019. Evaluation of thermal environment by coupling CFD analysis and wireless-sensor measurements of a full-scale room with cooling system. *Sustainable cities and society*, 45,

395-405.

- <sup>33</sup> Posner, J. D., Buchanan, C. R., & Dunn-Rankin, D., 2003. Measurement and prediction of indoor air flow in a model room. *Energy and buildings*, 35(5), 515-526.